Time-dependent isotache behaviour observed in physical soil-pipe interaction model tests – its practical implications on pipeline performance evaluation

C.K. Wong, R.G. Wan, & R.C.K. Wong
Department of Civil Engineering, Schulich School of Engineering – University of Calgary, Calgary, Alberta, Canada

ABSTRACT
Pipelines for the transport essential natural resources are often constructed at shallow depths through different geologic terrains. Permanent ground deformations can occur in actively moving slopes, landslides, surface faulting and ground subsidence, which impose external load on buried pipes. Large strains may be accumulated in the buried pipes and may affect their performance over time. The external load exerted on the pipe by the ground movement is dependent on the soil resistance mobilized in soil-pipe interaction. Recent available pipeline design guidelines (e.g., American Lifelines Alliance (ALA) and Pipeline Research Council International (PRCI)) provide recommendations on soil ultimate resistances for different soil types in drained and undrained loading conditions. However, these guidelines do not consider the effect of soil displacement rate on the soil ultimate resistance in soil-pipe interaction. This paper proposes to use the concept of "isotache" behavior to quantify the relationship between the soil-pipe relative displacement rate and the soil ultimate resistance on the pipe in compacted clays. The relationship is developed based on results measured in physical soil-pipe interaction models. Practical examples are presented to illustrate the use of this relationship to evaluate the performance of buried pipelines subjected to short- and long-term ground movements.

RÉSUMÉ
Le transport des ressources naturelles est effectué par des pipelines qui sont souvent enfouis à de faibles profondeurs, traversant différents terrains géologiques. Des déformations permanentes du sol peuvent se produire dues à des pentes en mouvement actif, aux glissements de terrain, les failles de surface et les affaissements du sol, qui imposent une charge externe sur la structure (pipeline). De grandes déformations peuvent s'accumuler et ainsi nuire à la performance de la structure au fil du temps. La charge externe exercée sur la structure par le mouvement du sol dépend de la résistance du sol mobilisée dans l'interaction sol-structure. Les directives récentes sur la conception des pipelines (par exemple, American Lifelines Alliance (ALA) et Pipeline Research Council International (PRCI)) fournissent des recommandations sur les résistances ultimes des sols pour différents types de sol dans des conditions de chargement drainé et non drainé. Cependant, ces directives ne considèrent pas l'effet de la vitesse de déplacement du sol sur la résistance ultime du sol dans l'interaction sol-structure. Cet article propose d'utiliser le concept de comportement «isotache» pour quantifier la relation entre la vitesse de déplacement relatif sol-structure et la résistance ultime du sol sur la structure dans des argiles compactées. La relation est développée sur la base des résultats mesurés dans des modèles d'interaction physique sol-pipeline. Des exemples pratiques sont présentés pour illustrer l'utilisation de cette relation pour évaluer la performance de pipelines enterrés soumis à des mouvements de terrain à court et à long terme.

1 INTRODUCTION

Buried pipelines have been designed and used to transport essential natural resources such as oil, water and natural gas. They can navigate through different geological terrains. This includes pipelines buried at shallow depths in moving slopes. Pipelines which cross a potential moving slope can be subjected to long-term, non-recoverable ground movements. Permanent ground deformations along part of the pipeline length can cause the pipe to reach its yield capacity due to large strain accumulation over time. Thus, the effect of permanent ground deformations on buried pipelines is critical for their safety and structural integrity. Existing buried pipeline design guidelines by American Lifelines Alliance (ALA, 2001) and Pipeline Research Council International (PRCI, 2009) have identified three distinct permanent ground deformation types buried pipelines can be subjected to: (1) longitudinal (axial), (2) transverse, and (3) complex ground movements. In longitudinal (axial) ground movement, the unstable soil mass is oriented parallel to the pipe axis. Yielding of the pipe in longitudinal ground movements is due to pipe buckling. In transverse ground movement, the unstable soil mass is oriented orthogonally to the pipe axis. Yielding of the pipe in transverse ground movements is due to pipe bending. Complex ground movement includes a combination of longitudinal and transverse ground movement components. Complex ground movement can either occur as shallow planar slips or deep-seated movement. Yielding of the pipe due to complex ground movement is a combination of pipe buckling and bending. However, these guidelines do not consider the effect of soil displacement rate on the soil ultimate resistance in soil-pipe interaction. This paper examines the time-dependent behaviour observed in soil element, soil-interface and physical model tests on compacted clay, and proposes to use the concept of "isotache" behavior to quantify the relationship between the soil displacement rate and the soil

ultimate resistance on the pipe in soil-pipe interaction in compacted soil.

The first part of the paper presents literature reviews on the "isotache" concept and the existing buried pipeline design guidelines. Then, results obtained from tests including triaxial compression, direct shear and soil-pipe interaction tests are examined and interpreted using the "isotache" concept. The relationship between the soil displacement rate and the soil ultimate resistance on the pipe in soil-pipe interaction under different loadings are proposed, followed by concluding remarks.

2 LITERATURE REVIEW

2.1 "Isotache" Concept

Three important time-dependent phenomena existing in clay soil are creep, stress relaxation, and strain rate effect. Creep is the process when strain is increasing while a constant stress is being maintained to a clay sample. Stress relaxation is the process when stress is decreasing while maintaining a constant strain. Strain rate effect is the process where for a change in strain rate, the stress-strain behaviour changes from one unique curve to another unique curve. These unique curves as a function of strain rate are defined as "isotaches". Physically, "isotache" behaviour implies that there is a unique material response for a given strain rate. For an increase in strain rate, the stress response becomes stiffer (i.e., increase in stress towards a higher "isotache" curve). For a decrease in strain rate, a softening response occurs in the stress response. This phenomenon in clay is well documented in literature, e.g., Leroueil et al. (1985; 1988) and Leroueil (2006).

The "isotache" concept has been successfully used in interpreting long-time one-dimensional consolidation behaviour in world-wide clays. Leroueil et al. (1985; 1988) and Leroueil (2006) suggested that long-time one-dimensional (1D) consolidation behaviour of saturated soft clay is controlled by a unique relationship among the vertical effective stress, strain, and strain rate $\sigma' - \varepsilon_{vp} - \dot{\varepsilon}_{vp}$ or $\sigma' - \varepsilon_{vp} - t$ where t is the time. For a given $\dot{\varepsilon}_{vp}$, there exists a unique non-linear relationship of $\varepsilon_{vp} - ln\sigma'$ with a unique preconsolidation pressure $\sigma_p{}'$, illustrated in Figure 1. This unique relationship is denoted as "isotache" behavior. In addition, there exists a unique non-linear relationship of $\ln \dot{\varepsilon}_{vp} - \ln \sigma_p{}'$. Curves of $\varepsilon_{vp} - \ln \sigma'$ with varying $\dot{\varepsilon}_{vp}$ converge into a single master curve if the normalized ln σ'/σ$_p$' is used.

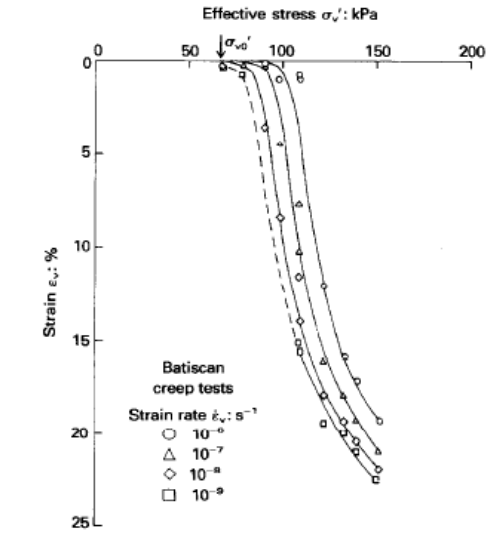

(a)

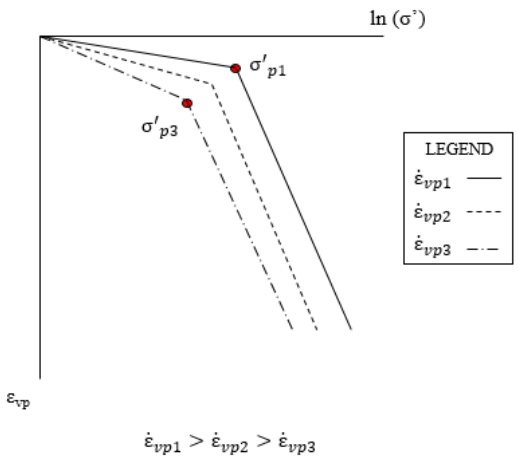

(b)

Figure 1. Illustration of the unique non-linear relationship between stress-strain-time or stress-strain-strain rate for soft clay. These relationships are known as isotaches. (a) 1D oedometer compression test results of vertical strain (ε_v) versus vertical effective stress (σ_v') on Batiscan clay illustrating isotaches (Leroueil et al. 1985), (b) Equivalent linear representation of isotaches by converting the effective stress scale to a semi-logarithmic scale (σ_{pi}' = preconsolidation pressure at strain rate $\dot{\varepsilon}_{vpi}$).

Watabe and Leroueil (2012) extended the use of the "isotache" concept and developed a three-isotache-parameters model to represent the variation of preconsolidation pressure with strain rate based on experimental data of world-wide clay samples:

$$\ln\left(\frac{\sigma_p' - \sigma_{pL}'}{\sigma_{pL}'}\right) = c_1 + c_2 \ln\left(\dot{\varepsilon}_{vp}\right) \quad [1]$$

where c_1 and c_2 are constants at a large strain rate ($\dot{\varepsilon}_{vp}$= 1 s^{-1}), and σ'_{pL} is the lower limit of the preconsolidation pressure at very small strain rate $\dot{\varepsilon}_{vp}$ close to 0. Watabe and Leroueil (2012) further developed an integrated fitting curve to normalize all the observed data of world-wide clay samples at a reference strain rate of $\dot{\varepsilon}_{vp0}$ = 1x10^{-7} s^{-1} (0.864%/day) which is close to the average strain rate attained in 24-hour-incremental loading consolidation oedometer tests. The σ'_p is defined as σ'_{po} at this reference strain rate. Then, c_1 = 0.935, σ_p'/σ_L'= 0.70, and by default c_2 = 0.107. In such case, the integrated curve passes the point ($\dot{\varepsilon}_{vp}$ = 1x10^{-7} s^{-1}, σ_p'/σ_0'= 1), and intersects at very small strain rate with a value of σ_p'/σ_L'= 0.70 (Figure 2a and 2b of semi-log and log-log plots, respectively). Therefore, the variation or relationship between the preconsolidation pressure and viscoplastic strain rate can be readily obtained from a standard 24-hour-incremental loading consolidation test in which the value of σ'_p is determined from the plot of e-ln(σ'). From Figure 2b, the slope value decreases from 0.009 to 0.074 with increasing strain rate from 1x10^{-14} to 1x10^{-4} s^{-1}.

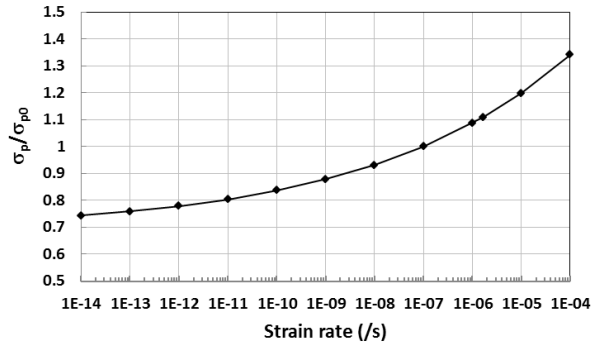

(a)

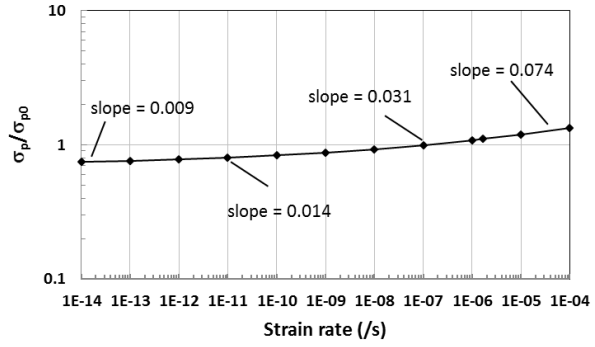

(b)

Figure 2. Integrated fitting curve – preconsolidation pressure is function of strain rate (a) semi-logarithmic plot (b) log-log plot (Watabe and Leroueil 2012), which can be approximated by $\frac{\sigma_p}{\sigma_{p0}} = 3.2\dot{\varepsilon}^{0.02}$.

2.2 Buried Pipeline Design Guideline Equations

The latest guidelines on shallow buried pipeline design, in ALA (2001) and PRCI (2009) contain a set of unique equations describing soil resistances against pipe movement in three different directions: longitudinal loading, vertical uplift loading, and transverse horizontal loading. All three equations are based on some form of a limit equilibrium analysis.

The longitudinal loading equation comprises two main components, a soil cohesion-dependent and a friction-dependent component:

$$T_U = \pi D\alpha c + \pi DH\bar{\gamma}\left(\frac{1+K_0}{2}\right)\tan\delta \quad [2]$$

where T_U is the maximum longitudinal (axial) soil force per unit of pipe transmitted to the pipe, D is the outside pipe diameter, α is a soil adhesion factor, c is the soil cohesion, H is the pipe embedment depth, $\bar{\gamma}$ is the effective soil unit weight, K_0 is the lateral earth pressure coefficient at-rest, and δ is the soil and pipe interface friction angle. By comparing closely with the Canadian Engineering Foundation Manual (2010), the longitudinal soil resistance equation is analogous to the design of a pile (deep) foundation.

The vertical uplift loading equation comprises two main components, a soil cohesion-dependent and a weight surcharge component:

$$Q_U = N_{cv}cD + N_{qv}\bar{\gamma}HD \quad [3]$$

where N_{cv} is a vertical bearing capacity factor for clay and N_{qv} is a vertical bearing factor for sand. Both N_{cv} and N_{qv} are dependent on the pipe embedment depth, H, and outer pipe diameter, D (ALA, 2001). Likewise, by comparing closely with the Canadian Engineering Foundation Manual (2010), the vertical uplift resistance equation is analogous to the design of a shallow foundation. Equation (3) can also be expressed in the following normalized form:

$$\frac{Q_U}{c_u D} = N_{cv}\frac{c}{c_u} + N_{qv}mD \quad [4]$$

where c_u is the soil unconfined shear strength, and is related to the soil cohesion by c_u = c/tan(45°-φ/2). The dimensionless parameter m is equal to $\gamma D/c_u$, which is a function of the soil unit weight and burial depth.

The transverse horizontal resistance equation comprises two main components, a cohesion-dependent and a weight surcharge component:

$$P_U = N_{ch}cD + N_{qh}\bar{\gamma}HD \quad [5]$$

where N_{ch} is a horizontal bearing capacity factor for clay and N_{qh} is a horizontal bearing capacity for sand. Both N_{ch} and N_{qh} are determined from empirical correlations (ALA 2001).

3 TIME-DEPENDENT OR "ISOTACHE" BEHAVIOUR OBSERVED IN TESTS

The material used is Regina clay, a dark brown highly expansive clay. The clay was obtained from an excavation site near Mosaic Stadium in Regina, Saskatchewan. Regina clay has an optimum water content at 28.5% with a dry density of 1500 kg/m^3. The clay content and liquid limit are 50% and 80%, respectively. The clay fraction comprises approximately 20-75% montmorillonite, 15-45% illite, and 10% kaolinite by mineralogy.

3.1 Consolidated Triaxial Compression Tests

Consolidated triaxial compression tests were conducted on compacted Regina clay samples to investigate the effect of strain rate on the strength-deformation characteristics. Samples were extracted at the conclusion of each of the physical model tests with Shelby tubes and trimmed to final dimensions of 120 mm in height and 60 mm in diameter. Two pieces of pre-treated No. 42 Whatman filter paper were placed on both ends of the sample to measure the matric suction. The apparatus for the consolidated triaxial compression test was the GDS triaxial testing machine. A finite confining stress (10 kPa and 50 kPa) was applied to the sample for 48 hours. After consolidation, the sample was sheared at varying displacement rates of 0.3 – 2 mm/day. Axial stress, axial strain, local axial and radial strains were recorded in the GDS acquisition system.

Figure 3 illustrates typical deviatoric stress-axial strain responses of compacted Regina clay sample RC4-1 in strain-controlled consolidated triaxial compression test. The compacted Regina clay sample exhibits non-linear hardening upon shearing with volumetric compaction. "Isotache" behaviour was clearly observed in the triaxial compression test. Physically, "isotache" behaviour implies that there is a unique material response for a given strain rate. For an increase in strain rate, the stress response becomes stiffer (i.e., increase in stress towards a higher "isotache" curve). For a decrease in strain rate, a softening response occurs in the stress response. In addition, another time-dependent phenomenon, relaxation was detected in the triaxial compression tests when the displacement rate was halted. In sample RC4-1 (Figure 3), the deviatoric stress drops from 216 to 146 kPa during stress relaxation at an axial strain of 0.062. The stress reduction is about 32%. The ultimate deviatoric stresses, q_f, at 6% axial strain for different strain rates were extrapolated from test data of sample RC4-1 and plotted against strain rate in Figure 4 of log-log plot. The data suggests a linear relationship with slope of m = 0.0434. This m-value falls within the range of 0.009 - 0.074 as shown in Figure 2b. This substantiates the validation of the normalization principle used in 1D consolidation behaviour in clay which is also applicable to time-dependent (viscous) behaviour due to strain rate effect in the triaxial compression on compacted Regina clay.

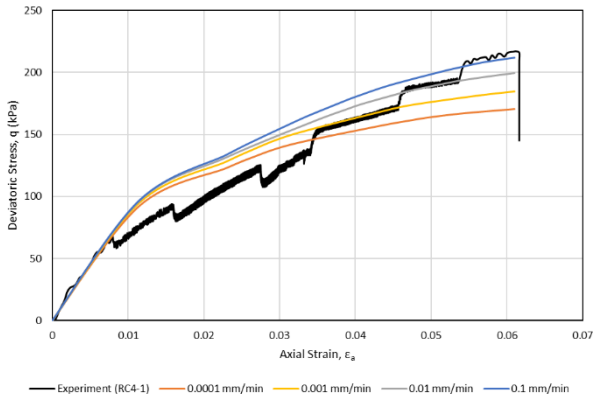

Figure 3: Deviatoric stress versus axial strain in consolidated triaxial compression test on Regina clay sample, RC4-1, at confining pressure of 10 kPa. The strain rates for ε_a = 0 – 0.01, 0.01 – 0.02, 0.02 – 0.03, 0.03 – 0.035, 0.035 – 0.045, 0.045 – 0.055, and 0.055 – 0.06 are 115%/day, 11.5%/day, 1.15%/day, 0.115%/day, 1.15%/day, 11.5%/day, and 115%/day, respectively. Comparison between the results from the triaxial test on sample RC4-1 and the isotaches generated using FEM with the creep and cap plasticity model. The Singh-Mitchell creep law was used in the creep model (Wong 2018).

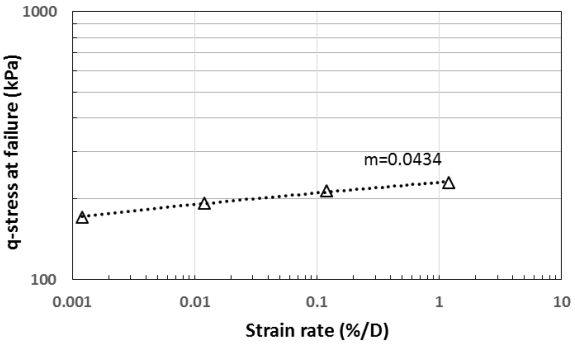

Figure 4. Plot of log(deviatoric stress at ultimate state) versus log(strain rate) for compacted Regina clay sample RC4-1.

Figure 3 also illustrates the comparison between the isotaches generated by the cap plasticity model in ABAQUS simulation (Dassault Systemes 2011) and the experimental result from the test of sample RC4-1. It can be seen that there is a relatively good fit between the experimental and numerical simulation results. Table 1 lists the values used for the cap plasticity model parameters in an attempt to match the test results of sample RC4-1.

Table 1. Cap model parameters used in ABAQUS simulation results on compacted Regina clay sample RC4-1. a) basic cap model inputs, b) cap hardening parameters, c) Singh-Mitchell creep law parameters for cap creep cohesion and consolidation sub-option inputs.
*The equation for the volumetric plastic strain in the cap plasticity model is: $\varepsilon_v^p = \frac{(\lambda-\kappa)}{(1+e_0)} \ln\left(\frac{p}{p_0}\right)$ where l = 0.2, k = 0.03, e_0 = 0.93and p_0 = 30 kPa.

a)

Parameter	Value
Material cohesion (kPa)	150
Material friction angle (°)	42
Cap eccentricity	0.01
Initial yield surface position	0
Transitional surface radius	0
Flow stress ratio	1

b)

Yield stress (kPa)	Volumetric plastic strain
30	0
70	0.074632
110	0.114445
150	0.141764
190	0.162586
230	0.179414
270	0.193538

c)

Parameter	Value
A	3×10^{-5}
α	5×10^{-5}
t_1	0.001
m	0.65

3.2 Direct shear box tests

The apparatus for the direct shear box test comprises the GeoTest S2215 direct shear machine and a brass shear box. The conventional brass shear box setup was used for the direct shear tests. The two halves used were ones with circular holes (60 mm in diameter). Once the two halves were assembled with a pair of set screws, a definitive mass of dry Regina clay was mixed with water until a desired water content was attained. The freshly mixed soil was then compacted using a metal cylinder inside the conventional shear box setup before being placed into the GeoTest S2215 direct shear machine. A normal confining stress of 30 -150 kPa was applied to the sample and allowed to consolidate for a period of 48 hours. After the equilibrium, the sample was sheared in varying rates of 0.003 – 0.053 mm/day. The responses under direct shearing such as horizontal shear force, vertical and horizontal displacements were monitored. At the end of the test, the sample matric suction was measured using a suction probe.

Figure 5 shows a typical test result of a direct shear test on compacted Regina clay sample DS3. The shear strength increases with increasing shear displacement. “Isotache” trend was observed in this test. The rate of shearing displacement has some impact on the shearing behaviour, i.e., the stiffness and shear strength decrease with decreasing displacement rate. This rate effect is illustrated in Figure 6. The slope of this log-log plot lies within the range of the integrated curve of Figure 2b, which supports the rate effect on the pre-consolidation pressure.

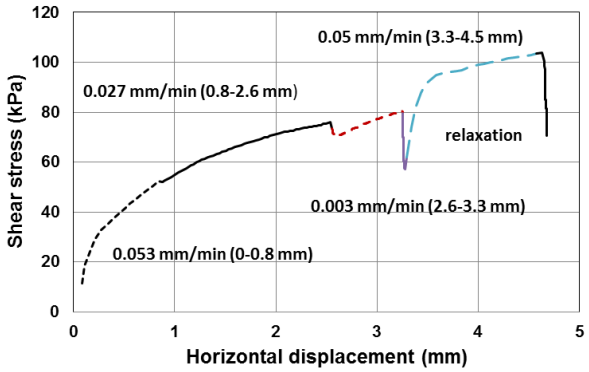

Figure 5: Shear stress versus horizontal displacement in direct shear test of Regina clay consolidated at 100 kPa (water content = 27%; bulk density = 1970 kg/m^3, matric suction = 20 kPa by suction probe).

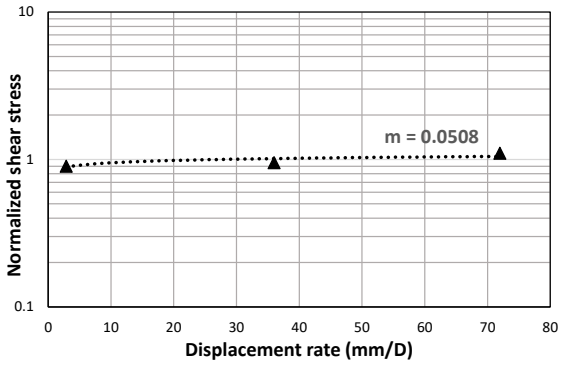

Figure 6. Plot of log(normalized shear stress at ultimate state) versus log(shear displacement rate) – results of direct shear test DS3 on compacted Regina clay.

3.3 Interface Tests Between Regina Clay and Pipe Steel

An integral component to solving the problem of soil and buried pipeline interactions is to understand the interface behavior between the soil and the steel surface of the pipe. To achieve this objective, one set of direct shear box tests were conducted to simulate this interface behavior. The

main parameters of interest from these tests are the peak and residual values of interface friction angle and interface adhesion. Instead of a conventional shear box setup with both brass shear box halves having a hole, only the top half was kept with the bottom half being replaced with a solid steel plate with a rough surface. Both the top half and the solid steel plate were assembled with a pair of set screws. A definitive mass of dry Regina clay was mixed with water until a desired water content was attained. The freshly mixed soil was then compacted inside the modified shear box setup. The GeoTest S2215 direct shear machine was the apparatus used to conduct the soil-steel interface tests with the modified shear box setup. The shearing rates varied from 0.002-0.1 mm/min.

Figure 7 plots the response of the soil-steel interface at a confining stress of 100 kPa. A peak strength was mobilized at a shear displacement of about 1.2 mm. The shear strength was gradually degraded to a residual strength with increasing displacement. The rate effect was not tested in the pre-peak regime as the shear displacement prior to the peak strength was small. The shear rate was varied in the softening regime. The effect on the change in shear strength could not be delineated as the effects of both strength softening and rate dependency could take place simultaneously. However, stress relaxation did occur when no shear displacement was applied to the test. This shows that the rate effect does play an important role in the response of soil-interface under direct shearing.

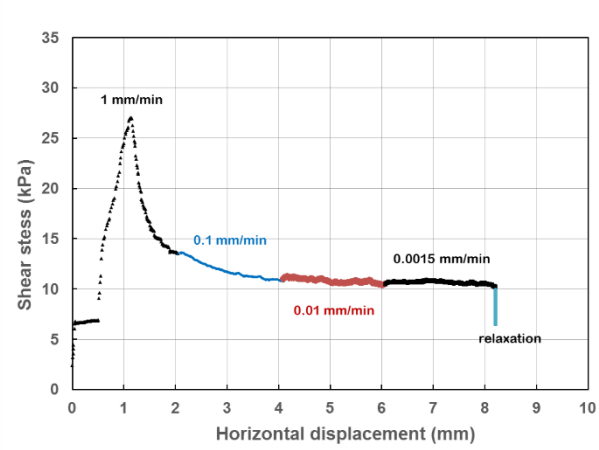

Figure 7. Shear stress versus horizontal displacement in direct shear test of Regina clay-steel sample consolidated at 40 kPa (water content of 25%).

3.4 Soil-Pipe Interaction Physical Model Tests

Physical model tests were carried out to determine three distinct soil resistances or springs against different loading directions specified in the buried pipeline design guidelines of ALA (2001) and PRCI (2009). They include longitudinal (axial) soil springs, vertical uplift soil springs, and transverse horizontal (lateral) soil springs. Test details and results of these three loading types: longitudinal (axial) (LA) loading tests, vertical uplift (VU) loading tests, and transverse horizontal (TH) loading tests, are highlighted herein.

Two experimental setups were used in this study. A rectangular steel box with dimensions of 2.4 m by 0.9 m in the long axis and a square cross section of 0.9 m x 0.9 m was used to conduct longitudinal (axial) (LA) and vertical uplift (VU) loading tests. A steel pipe was buried in compacted soil mass inside the box and displaced relatively to the fixed box at varying displacement rates using hydraulic rams driven by step motors. Load cells and displacement transducers were used to monitor the forces and displacements on the buried pipe. A circular steel tank of 1.5 m in diameter and 1.2 m in height was used to conduct longitudinal (axial) (LA) and transverse horizontal (TH) loading tests. Partitions inside the tank was allowed to mimic plane-strain condition. The tank was mounted on a movable steel frame resting on two sets of wheels and rails. In longitudinal loading tests, the buried pipe was displaced against the frame using a step motor. In transverse horizontal (TH) loading tests, the buried pipe was pinned at both ends using steel blocks anchored to the floor. The tank resting on the steel frame was displaced using the step motor at specific rates. Details of test setup and instrumentation are presented by Wong (2018).

For the compaction of Regina clay in the physical model tests, however, it was decided the soil water content was set at 30%, approximately 2% wet of optimum. This was to ensure easier compaction within the test apparatus while achieving a relatively high dry density simultaneously (85%-90% of the maximum dry density). The soil, as result, was moisture conditioned to 30% and then placed in steel barrels. Each barrel with the moisturized soil had a mass of 200 kg each. The barrels were then emptied into the rectangular box or the circular tank, and the loose clumps of wet Regina clay were compacted in 150 mm (6”) layers using a custom-made wooden compactor in the box and a pneumatic backfill tamper in the tank, respectively. The wooden compactor was made of a wooden crate with two pieces of plywood bolted onto the crate. Verification of the compacted dry density with the expected dry densities was conducted with a nuclear densitometer after several soil layers were filled at one time. In addition, samples were extracted at the end of the test using 62.5 mm (2.5”) diameter Shelby tubes to check for compacted bulk and dry densities.

3.4.1 Longitudinal loading tests

Two sets of longitudinal loading tests were conducted, one with the rectangular box, the other with the circular tank. The objective of both tests was to determine the maximum longitudinal subgrade reaction (soil resistance).

Figure 8 presents the force-displacement response in the longitudinal loading test LA1, conducted in the rectangular box. The 150-mm pipe was buried at a depth ratio of H/D = 3. The maximum subgrade reaction in this test (LA1) was 1.9 kN/m at a longitudinal displacement of approximately 2.5 mm. The total cumulative axial displacement in this test was 9 mm. This test was conducted with three different displacement rates of 0.3, 1, and 2 mm/day, and with four stress relaxation phases. The change in soil resistance due to a change in the

displacement rate was the largest from 4.5 to 5.5 mm of axial displacement in stage S7. The rate changed from 1 mm/day to 0.3 mm/day, resulting in a drop of 0.1 kN/m in soil resistance. The highest amount of stress relaxation occurred in the first relaxation phase (stage S2), where the subgrade reaction resistance dropped by 0.7 kN/m, a drop in longitudinal loading by 40%.

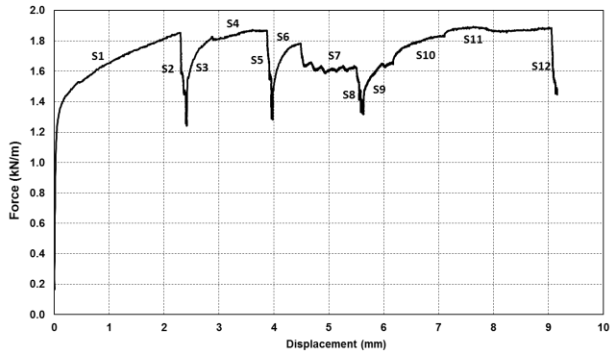

Figure 8. Longitudinal (axial) displacement test LA1, (H/D = 3) on compacted Regina clay conducted on the Golder rectangular box (H/D =3) – The pipe displacement rate and magnitude are: S1, S3, S11 – 1.87, 1.72, 1.66 mm/day, S2, S5, S8, S12 – relaxation, S4, S6, S10 – 1 mm/day, S7, S9 – 0.2 mm/day.

Figure 9 illustrates the force-displacement response in the longitudinal loading test LA2 conducted in the circular tank. The maximum subgrade reaction in this test (LA2) was 8.5 kN/m at a longitudinal displacement of approximately 0.4 mm. The subgrade reaction eventually settled towards a residual value of 3.5 kN/m after 6 mm of longitudinal displacement. The total cumulative axial displacement in this test was 9.5 mm. This test was conducted with various displacement rates ranging from 0.04 to 20.5 mm/day and with one stress relaxation phase. The change in soil resistance due to a change in the displacement rate was the largest from 1 to 3.5 mm of axial displacement (stages S1 and S2). The rate changed from 20 mm/day to 2 mm/day, resulting in a drop of 2.5 kN/m in soil resistance. The amount of stress relaxation in the only relaxation phase (stage S11), was a drop of 0.6 kN/m in longitudinal loading, a drop in longitudinal loading by 17%. It is also noted in test LA2, a peak resistance has been mobilized followed by a drop towards a residual resistance, whereas the test LA1 only showed gradual hardening-type behavior. The contrasting magnitude of both tests, in terms of the maximum subgrade reaction and stress drop during relaxation may be attributed to the difference in the effort and consistency in the soil compaction process in the two tests. With manual compaction completed in the test LA1 conducted in the rectangular box, the void space surrounding the bottom arc of the pipe surface might not necessarily be filled and compacted properly compared to that in the test LA2. This might result in a smaller contact area between the soil and the pipe, leading to a lower maximum resistance value in test LA1. In addition, the amount of energy for each blow could vary in manual compaction, leading to inconsistencies in the resulting bulk and dry densities. For the test conducted in the circular tank, soil compaction was completed using the pneumatic tamper. The finite quantity of air pressure injected for the tamper to be operational resulted in consistent, repetitive compaction strokes. However, the energy per blow using the pneumatic tamper could be high enough to over densify the soil in comparison to manual compaction, possibly leading to stiffer soil resistances. It is interesting to note that the response observed in test LA2 is comparable to that observed in the soil-interface test, both displaying peak and residual trends.

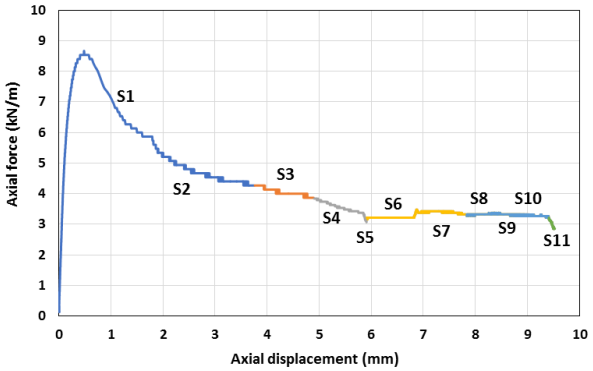

Figure 9. Longitudinal (axial) displacement test LA2, (H/D = 3) on Regina clay conducted on the University of Calgary circular tank (H/D =3). The pipe displacement rate and magnitude are: S1 – 20.51 mm/day (0 – 1.9 mm); S2 – 2.23 mm/day (1.9 – 3.8 mm); S3 – 1.10 mm/day (3.8 – 4.9 mm); S4 – 0.28 mm/day (4.9-5.9 mm); S5 – relaxation 1; S6 – 22.11 mm/day (5.9 – 6.9 mm); S7 – 0.09 mm/day (6.9-7.4 mm); S8 – 1.05 mm/day (7.4-7.9 mm); S9 – 0.04 mm/day (7.8-8.1 mm); S10 – 1.67 mm/day (8.1 – 9.4 mm); S11 – relaxation 2.

3.4.2 Vertical uplift loading tests

Vertical uplift loading tests were conducted on compacted Regina clay using the rectangular box. The objective of the tests was to determine the maximum vertical uplift subgrade reaction.

Figure 10 illustrates the average force-uplift displacement response of test VU1. The 150-mm pipe was buried at a depth ratio of H/D = 3. The maximum average subgrade reaction in the test VU1 was 17.8 kN/m at an uplift displacement of approximately 3.2 mm. The total average cumulative vertical uplift displacement in this test was 7.7 mm. The original data readings on the uplift force and uplift displacement in this test was measured by two separate load cells and displacement transducers placed on either end of the pipe in the test. As a result, the average values were based on the average readings of the two sets of instrumentation. Test VU1 was conducted with three different displacement rates of 0.3, 1, and 2 mm/day, and with four stress relaxation phases. The change in soil resistance due to a change in the displacement rate was the largest from 5.8 to 6.8 mm of vertical uplift

displacement during stage S10. The rate changed from 0.3 mm/day to 1 mm/day, resulting in an increase of 1 kN/m in soil resistance. The highest amount of stress relaxation occurred in the first relaxation phase (stage S2), where the subgrade reaction dropped by 5.8 kN/m, a drop in vertical uplift loading by 33%.

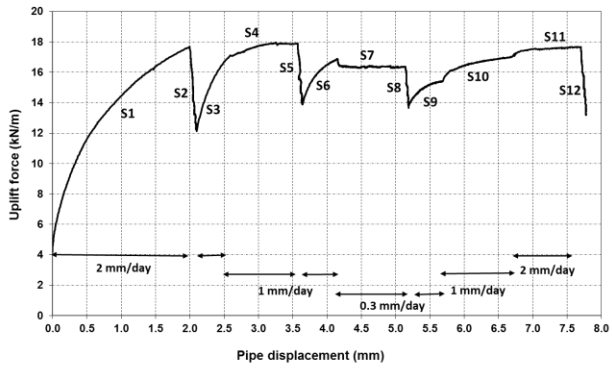

Figure 10. Vertical (uplift) displacement test VU1, (H/D = 3) – Average uplift force versus pipe displacement. The pipe displacement rate and magnitude are: S1, S3, S11 – 1.87, 1.72, 1.66 mm/day; S2, S5, S8, S12 – relaxation; S4, S6, S10 – 1 mm/day; S7, S9 – 0.2 mm/day.

3.4.3 Transverse horizontal loading tests

Transverse horizontal loading tests were conducted using the circular tank. The objective of these tests was to determine the maximum transverse horizontal subgrade reaction.

Figure 11 illustrates the force-displacement response in the transverse horizontal loading test TH2. The 150-mm pipe was buried at a depth ratio of H/D = 3. The maximum horizontal subgrade reaction in this test was 36.0 kN/m at a transverse horizontal displacement of approximately 29 mm which are much larger than those observed in longitudinal and vertical uplift loading tests. The total cumulative transverse horizontal displacement in this test was 40 mm. This test was conducted with various displacement rates ranging from 0.2 mm/day to 16.7 mm/day, one unloading-reloading cycle (stages S7 and S8), and one stress relaxation phase at stage S6. The amount of stress relaxation occurred was a drop in transverse horizontal load by 6.6%, corresponding to a subgrade reaction resistance dropped of 2.1 kN/m. The change in soil resistance due to a change in displacement rate was noticeable in the test TH2, illustrating the "isotache" phenomenon. For example, the largest change in soil resistance in the second test occurred from stage S4 to S5, where a drop of 1 kN/m occurred when the displacement rate dropped from 0.96 mm/day to 0.17 mm/day.

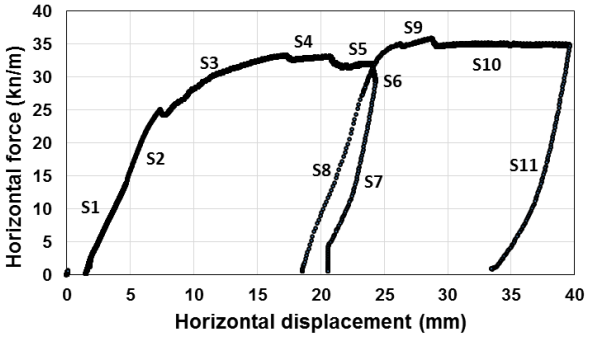

Figure 11. Transverse (horizontal) displacement test TH2 (H/D = 3, plane strain loading). The pipe displacement rate and magnitude are: S1 – 3.16 mm/day (0 – 4.95 mm) S2 16.72 mm/day (4.95 -7.41 mm); S3 – 2.62 mm/day (7.4 1– 17.45 mm); S4 – 0.96 mm/day (17.45 – 21.0 mm); S5 – 0.17 mm/day (21.0 -23.9 mm), S6 – relaxation; S7 – unload at 28.19 mm/day; S8 – reload at 288.1 mm/day; S9 – 52.6 mm/day (22.8 - 33.3 mm); S10 – 2.89 mm/day (28.2 – 39.5 mm) relaxation 2; S11 – unload.

The soil ultimate resistance values at varying displacement rates for all physical soil-pipe prototype tests in this study were extrapolated by tracing isotaches (hyperbolic) patterns and plotted in Figure 12 of log-log plot. The soil ultimate resistance is analogous to the deviatoric stress at failure, q_f, and the displacement rate is analogous to the strain rate, $\dot{\varepsilon}_{vp}$ in triaxial compression. The relationships display linear trends in log-log plot, and their slope values are illustrated in the same plot. The values of the slope fall in a range of 0.030 - 0.089, which are consistent with the range shown in Figure 2b. This observation validates the normalization principle in 1D constant rate of strain tests suggested by Leroueil et al. (1985).

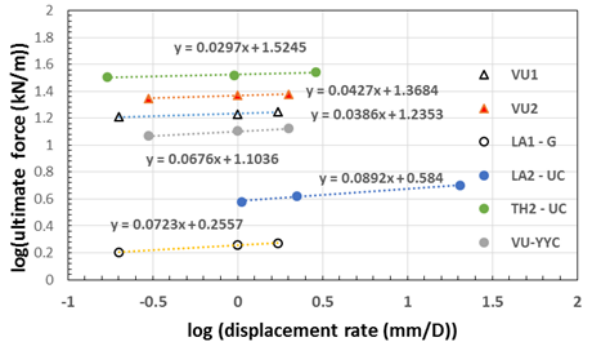

Figure 12. Determination of slope of plots of log(ultimate force) versus log(displacement rate) for vertical uplift, transverse displacement and axial loading tests in compacted Regina clay and Calgary till.

4 DISCUSSION

The test results and analysis based on this study show that the soil ultimate resistances mobilized in soil-pipe interaction under different loadings increase with the relative displacement rate between the pipe and the surrounding soil following the "isotache" behaviour. The variation of ultimate shear strength q_f or soil-interface resistance Q with strain rate $\dot{\varepsilon}$ or displacement rate $\dot{\delta}$ in element tests (consolidated triaxial compression and direct shear) and soil-interface and soil-pipe interaction tests, respectively may be expressed as:

$$\frac{dq_f}{d\dot{\varepsilon}} = \frac{\partial q_f}{\partial c}\frac{dc}{d\dot{\varepsilon}} + \frac{\partial q_f}{\partial \varphi}\frac{d\varphi}{d\dot{\varepsilon}} \quad [6]$$

$$\frac{dQ}{d\dot{\delta}} = \frac{\partial Q}{\partial c}\frac{dc}{d\dot{\delta}} + \frac{\partial Q}{\partial \varphi}\frac{d\varphi}{d\dot{\delta}} \quad [7]$$

Based on the work by Sheahan et al. (1996), it is reasonably postulated that the cohesion component is viscous rate-dependent and the friction component is independent of rate effect. Bishop and Henkel (1962) reported that in consolidated drained triaxial compression tests on clay, a tenfold increase in the time to failure results in a decrease of shear strength about 5%. This value is comparable to the slope values determined in our tests (Figures 4, 6 and 12). It is important to understand the variation rate depends on the cohesion characteristic which is function of clay type, clay content and stress history.

The viscous (rate-dependent) behaviour is not considered in the existing buried pipeline design guidelines. The typical slope movement rates occurred in Alberta vary in between 25 mm/y and 480 mm/y depending on site location and precipitation (Song et al. 2006). It is of practical significance for the pipeline industry to be able to continually assess pipeline performance in areas with unstable soil movements and to perform necessary remediation procedures such as pipe stress relief to prolong pipeline operation at the right time. To include the "isotache" behaviour in the design and analysis of soil-pipe interaction in buried pipelines, two important aspects must be addressed: (i) relation between the slope movement rate and the soil-pipe relative displacement rate, and (ii) drainage condition in the field.

The slope movements are commonly monitored using slope indicators and surface monuments. It is critical to translate these data to the soil-pipe relative displacement. The soil displacement profile along the depth of the soil mass slip must be estimated, and the displacement components in longitudinal and transverse directions are resolved based on the pipe alignment with respect to the soil resultant movement direction.

With the estimated soil-pipe relative displacement, one need to determine if the loading is in undrained or drained condition during soil deformation. According to PRCI (2009), the cohesion and friction angles embedded in equation [2] to [5] are effective or drained parameters. Effective stress analysis should be conducted in soil-pipe interaction. In case of fast loading rate, excess pore pressure buildup could develop in soil around the pipe during soil deformation, and the effective confining stress around the pipe would decrease resulting in a decrease in the shear strength. In case of slow loading rate, consolidation of soil occurs during soil deformation allowing dissipation of excess pore pressure. The variation of shear strength depends on the loading rate, soil coefficient of consolidation, and drainage path (burial depth). In the state-of-practice, soil undrained shear strength is used in a total stress analysis of soil-pipe interaction for low permeable clay, and the effect of the rate of pipe movement is not considered. The soil ultimate resistances mobilized in undrained condition are lower than those mobilized in drained condition because of the excess pore pressure buildup under fast loading rate. The dependency of rate on the shear strength illustrated in this study is solely attributed to the time-dependent viscous behaviour of soil occurred under fully drained conditions. This behaviour is not considered in PRCI (2009) at all. To assess occurrence of such drained behaviour in the field, one must ensure the relative displacement rate between a pipe and the surrounding soil is sufficiently small that the rate of excess pore pressure is balanced by the rate of consolidation during soil deformation. A simple criterion by normalizing the displacement rate *v* with the pipe diameter *D* and the coefficient of consolidation c_v is proposed in PRCI (2009): $V_n = vD/c_v$ and $V_n < 0.1$ for drained condition. This criterion is limited to transverse loading and shallow burial depth. In addition, the pore pressure A- and B-parameters are not taken into account.

For undrained condition, the rate-dependent undrained shear strength of soil may be used in soil-pipe interaction based on the total stress α-method used in pile foundation design. For drained condition, the rate-dependent drained shear strength parameters of soil should be used in those equations for soil ultimate resistances recommended by PRCI (2009), i.e., equations [2] to [5]. The soil total resistance is derived from both cohesion and friction components. Using the principle of similitude, the soil ultimate resistances mobilized in soil-pipe interaction in buried pipes would follow the "isotache" relationship illustrated in Figure 12. With given shear displacement rates in the field, the change in the soil ultimate resistance from Q_2 to Q_1 can be estimated from the following log-log relationship.

$$\log\left(\frac{Q_2}{Q_1}\right) = m\log\left(\frac{\dot{\delta}_2}{\dot{\delta}_1}\right) \quad [8]$$

For illustration, if the soil-pipe relative displacement is increased from $\dot{\delta}_1$ = 25 mm/y to $\dot{\delta}_2$ = 480 mm/y, the increase in the soil resistance is about 15.9% with m = 0.05. The strain or stress exerted on the pipe would be increased by the amount percentage if the pipe is within the elastic limit.

5 CONCLUDING REMARKS

Consolidated triaxial compression, direct shear, soil-interface and soil-pipe model tests were conducted to investigate the time-dependent viscous (rate-dependent) behaviour of compacted Regina clay. "Isotache" behaviour were detected in the tests. Physically, "isotache" behaviour implies that there is a unique material response for a given strain rate. For an increase in strain rate, the stress

response becomes stiffer (i.e., increase in stress towards a higher “isotache" curve). For a decrease in strain rate, a softening response occurs in the stress response. A methodology is proposed to estimate the variation of soil ultimate resistance mobilized in soil-pipe interaction for buried pipelines with soil movement rate, which is not considered in the existing buried pipeline design guidelines (ALA 2001; PRCI 2009).

6 ACKNOWLEDGEMENT

The authors appreciate the support provided by the Natural Science and Engineering Council of Canada (NSERC), TransCanada Limited, and University of Calgary.

7 REFERENCES

American Lifelines Alliance (ALA). 2001. Guidelines for the design of buried steel pipe. www.americanlifelinesalliance.org.

ASTM. 2012. *Standard test methods for laboratory compaction characteristics of soil using standard effort (12 400 ft-lbf/ft^3 (600 kN-m/m^3))*. American Society for Testing and Materials International, West Conshohocken, Pennsylvania, USA. ASTM D698-12e2.

Bishop, A.W. and Henkel, D.J. 1962. *The measurement of soil properties in the triaxial test*. E. Arnold, London, UK, 228 pages.

Canadian Geotechnical Society. 2010. *Canadian Engineering Foundation Manual*. 5th edition. Altona, Manitoba, Canada: Friesens Corporation.

Dassault Systemes (2011). Abaqus FEA, version 6.11. Dassault Systemes S.A., Velizy- Villacoublay, France.

Leroueil, S., Kabbaj, M., Tavenas, F., and Bouchard, R. 1985. ‘Stress–strain–strain-rate relation for the compressibility of sensitive natural clays. *Geotechnique,* 35(2): 159–180.

Leroueil, S. (2006). The isotache approach - where are we 50 years after the development by Professor Suklje? In Proceedings of the 13th Danube-European Conference on Geotechnical Engineering, Slovenian Geotechnical Society, pp. 55-88.

Leroueil, S., Kabbaj, M. and Tavenas, F. 1988. Study of the validity of a σ_v'-ε_v-$\dot{\varepsilon}_v$ model in in situ conditions. *Soils and Foundation*, 28(3): 13-25.

Pipeline Research Council International (PRCI). 2009. *Extended model for pipe soil interaction*. Catalog No. L51990.

Sheahan, T. C., Ladd, C. C., and Germaine, J. T. 1996. Rate-dependent undrained shear behavior of saturated clay. *Journal of Geotechnical Engineering*, 22(2): 99–108.

Song, B., Cheng, J. R., Chan, D. H. and Zhou, J. 2006. Numerical simulation of stress relief of buried pipeline at Pembina river crossing. In Proceedings of the 2006 International Pipeline Conference, September 25-29, 2006, Calgary, Alberta, Canada: ASME, pp. 325-334.

Watabe, Y. & Leroueil, S. 2012. Modelling and implementation of the isotache concept for long-term consolidation behavior. *International Journal of Geomechanics*, A4014006.

Wong, C.K. 2018. Physical and numerical modelling of pipelines in elastic visco-plastic soils under long-term ground movements. PhD thesis, Department of Civil Engineering, University of Calgary, Calgary, Alberta, Canada, 233 pages.